ISSN (Print) 1226-1750
ISSN (Online) 2233-6656
Journal of Magnetics 21(2), 235-238 (2016) http://dx.doi.org/10.4283/JMAG.2016.21.2.235

Synthesis, Structure and Magnetization Behaviors of $MnBi/Fe_3B/Nd_2Fe_{14}B$ Nanocomposite alloy

Y. Yang, Q. Wu, Y. C. Hu, P. Y. Zhang, and H. L. Ge*

China Jiliang University, Magnetism Key Laboratory of Zhejiang Province, 310018 Hangzhou, China

(Received 28 December 2015, Received in final form 4 March 2016, Accepted 24 March 2016)

Microstructure and magnetization behaviors of $MnBi/Fe_3B/Nd_2Fe_{14}B$ nanocomposite alloy have been investigated. It was found that the coercivity increased firstly and then decreased, and saturation magnetization decreased with the additon of MnBi alloy. The addition of 40 wt.% MnBi powder enhanced the coercivity from 192.8 kA/m to 311.2 kA/m. The δM and D(H)-H plots suggested the occurrence of a stronger exchange-coupling occurring between the hard and soft magnetic phase for this sample. The dependence of coercivity with temperature was discussed in 40 wt.% $Mn_{55}Bi_{45}$/ 60 wt.% $Nd_{4.5}Fe_{76.5}Nb_{0.5}B_{18.5}$ alloy powder, and a positive temperature coefficient was founded from 298 K to 350 K.

Keywords : nanocomposite alloy, coercivity, exchange coupling interaction

1. Introduction

$Fe_3B/Nd_2Fe_{14}B$-type nanocomposite permanent magnets [1, 2] have been attracting considerable attention because of the relatively low rare earth contents and reasonably high magnetic performances. However, its relatively low magnetic anisotropy limits the improvement of its $(BH)_{max}$. Previous studies have shown that the addition of hard magnetic phase can enhance the coercivity and $(BH)_{max}$ of composite magnets[3]. MnBi with a hexagonal NiAs structure (low-temperature phase, LTP) has a high magnetocrystalline anisotropy and positive temperature coefficient of coercivity and has potential as a "rare-earth free" hard magnet [4-6].

To further enhance the coercivity of $Fe_3B/Nd_2Fe_{14}B$-based nanocomposite alloys, $MnBi/Fe_3B/Nd_2Fe_{14}B$ nanocomposite alloy were prepared in this paper, and the effects of addition of MnBi on microstructure and magnetization behaviors of $Fe_3B/Nd_2Fe_{14}B$-based nanocomposite alloy has been investigated.

2. Experimental Details

The original alloy with nominal composition of $Nd_{4.5}Fe_{76.5}Nb_{0.5}B_{18.5}$ was prepared by the strip casting (SC) technique, using the 99.9 wt.% Nd, Fe, Nb and FeB alloy with 19.78 wt.% B content as raw materials. Tangential velocity of the wheel surface (v_s) set at 5 m/s. MnBi ingots with nominal composition of $Mn_{55}Bi_{45}$ were prepared by arc melting technique. The obtained button ingots were crashed and re-melted for composition uniformity. $Nd_{4.5}Fe_{76.5}Nb_{0.5}B_{18.5}$ and $Mn_{55}Bi_{45}$ powder were mixed by high-energy ball milling.

The phase composition was examined by X-ray diffraction (XRD). Magnetic measurements were accomplished by using a vibrating-sample magnetometer (VSM) with a maximum applied field of 2.0 T.

3. Results

Figure 1 shows the XRD patterns for x wt.% $Mn_{55}Bi_{45}$/ (1-x) wt.% $Nd_{4.5}Fe_{76.5}Nb_{0.5}B_{18.5}$ (x = 0, 20, 40, 60) alloy powder. Only $Nd_2Fe_{14}B$, Fe_3B and α-Fe phases are observed in the sample without $Mn_{55}Bi_{45}$ alloy. LTP MnBi and Bi phases accompanied by $Nd_2Fe_{14}B$, Fe_3B and α-Fe phases are observed with the addition of $Mn_{55}Bi_{45}$ alloy. Furthermore, the diffraction peak position of each phase is not change for each sample. It is implied that the mix of $Mn_{55}Bi_{45}$ and $Nd_2Fe_{14}B$ alloy by high-energy ball milling does not affect their respective crystal structure. According to the XRD patterns, the grain size of LTP MnBi and $Nd_2Fe_{14}B$ phase is about 30 nm and 20 nm in

*Corresponding author: Tel: +13034206898
Fax: +0571-28889526, e-mail: hongliang_ge@cjlu.edu.cn

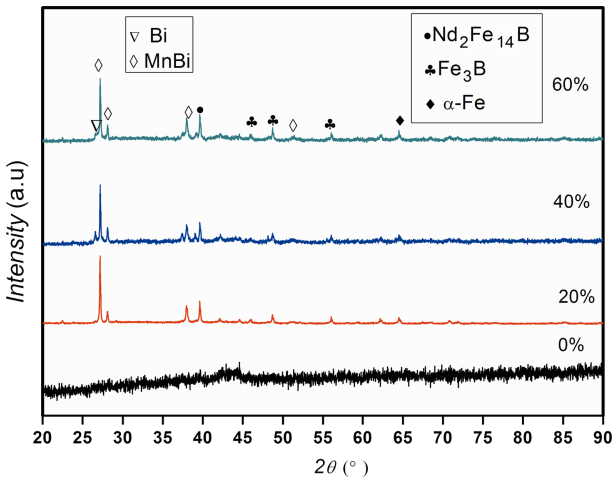

Fig. 1. (Color online) XRD patterns for x wt.% $Mn_{55}Bi_{45}$/(1–x) wt.% $Nd_{4.5}Fe_{76.5}Nb_{0.5}B_{18.5}$ (x = 0, 20, 40, 60) alloy powder.

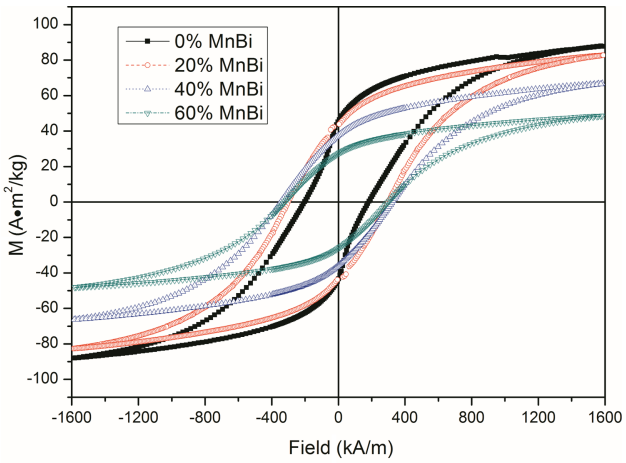

Fig. 2. (Color online) Magnetic hysteresis loops for x wt.% $Mn_{55}Bi_{45}$/(1–x) wt.% $Nd_{4.5}Fe_{76.5}Nb_{0.5}B_{18.5}$ (x = 0, 20, 40, 60) alloy powder.

these samples, respectively.

Magnetic hysteresis loops for x wt.% $Mn_{55}Bi_{45}$/(1–x) wt.% $Nd_{4.5}Fe_{76.5}Nb_{0.5}B_{18.5}$ (x = 0, 20, 40, 60) alloy powder are shown in the Fig. 2. It is noticed that the hysteresis loop of these samples exhibit a nearly single hard magnetic phase behavior and the coercivity increases firstly and then decreases with the $Mn_{55}Bi_{45}$ content as shown in the Fig. 3. The coercivity obviously increases from 192.8 kA/m to 311.2 kA/m with the $Mn_{55}Bi_{45}$ content is 40 wt.%. However, the decline in the coercivity is observed for 60 wt.% $Mn_{55}Bi_{45}$/40 wt.% $Nd_{4.5}Fe_{76.5}Nb_{0.5}B_{18.5}$. It can be seen from Fig. 3 that saturation magnetization keeps on decreasing with the additon of MnBi alloy, which is caused by relatively low magnetization of $Mn_{55}Bi_{45}$ alloy. The magnetic properties of ball milled $Mn_{55}Bi_{45}$ and

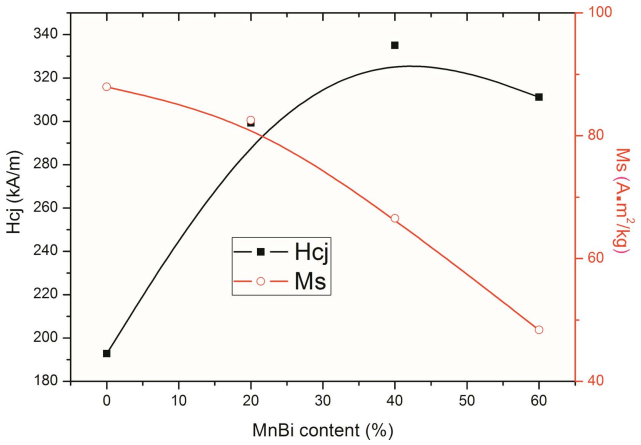

Fig. 3. (Color online) Coercivity and saturation magnetization dependence of MnBi content.

Table 1. Saturation magnetization (*Ms*), intrinsic coercivity (*Hcj*) of the single-phase $Mn_{55}Bi_{45}$ and $Nd_{4.5}Fe_{76.5}Nb_{0.5}B_{18.5}$ magnets.

Magnets	*Ms* (A·m²/kg)	*Hcj* (kA/m)
$Mn_{55}Bi_{45}$	25.4	1328.7
$Nd_{4.5}Fe_{76.5}Nb_{0.5}B_{18.5}$	87.96	192.84

$Nd_{4.5}Fe_{76.5}Nb_{0.5}B_{18.5}$ single alloy magnets are shown in Table 1.

To get further insight to the different magnetic behavior of these sample, the exchange coupling interaction between the soft and hard phases was estimated by δM plot [7, 8], which can be defined as $\delta M = m_d(H) - [1 - 2m_r(H)]$, where $m_r(H)$ is acquired after the application and subsequent removal of a direct field H and $m_d(H)$ is acquired after dc saturation in one direction and the subsequent application and removal of a direct field H in the reverse direction. The positive δM-peak height indicates the existence of exchange coupling interaction between the magnetic phases, the maximum δM value reflects the strength of exchange coupling interaction, and is generally obtained at the field around coercivity [9, 10]. Figure 4 shows the δM plots of x wt.% $Mn_{55}Bi_{45}$/(1–x) wt.% $Nd_{4.5}Fe_{76.5}Nb_{0.5}B_{18.5}$ (x = 0, 20, 40, 60). A positive δM is observed in all samples, confirming the existence of exchange coupling interaction between soft and hard phases. It is found that positive δM value increased by the addition of 20 wt.% and 40 wt.% MnBi alloy, which indicates that the exchange coupling interaction between the soft phase and hard phase enhances, leading to increasing of the coercivity. However, compared to 40 wt.% $Mn_{55}Bi_{45}$/60 wt.% $Nd_{4.5}Fe_{76.5}Nb_{0.5}B_{18.5}$, the smaller positive δM value is found in 60 wt.% $Mn_{55}Bi_{45}$/40 wt.% $Nd_{4.5}Fe_{76.5}Nb_{0.5}B_{18.5}$ alloy, indicating that more weak ex-

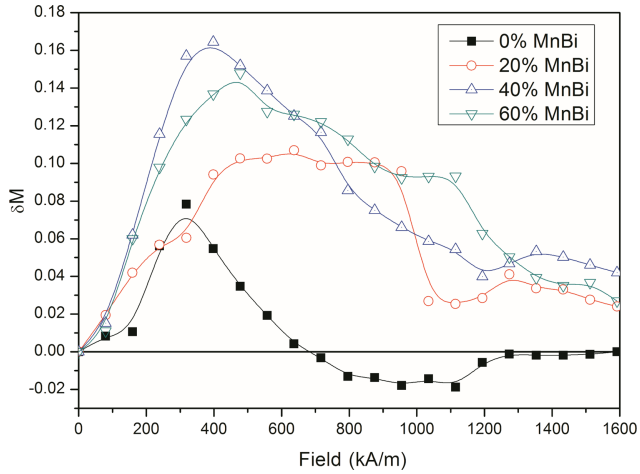

Fig. 4. (Color online) δM plots for x wt.% $Mn_{55}Bi_{45}$/(1−x) wt.% $Nd_{4.5}Fe_{76.5}Nb_{0.5}B_{18.5}$ (x = 0, 20, 40, 60) alloy powder.

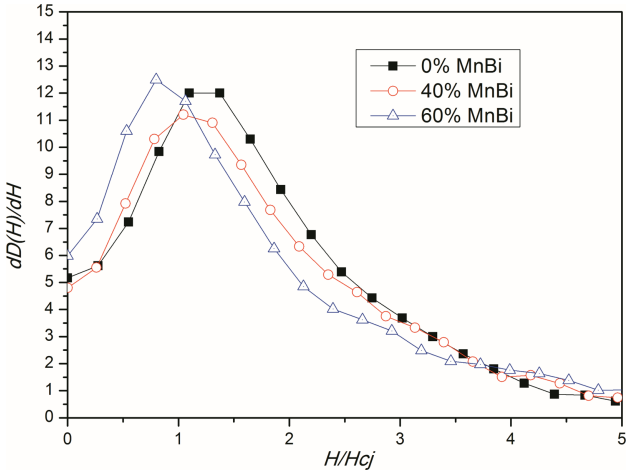

Fig. 5. (Color online) The d*D*(H)/dH-*H* curves for wt.% $Mn_{55}Bi_{45}$/(1−x) wt.% $Nd_{4.5}Fe_{76.5}Nb_{0.5}B_{18.5}$ (x = 0, 40, 60) alloy powder.

change coupling interaction with increasing the content of MnBi, resulting in deterioration of the hysteresis loop.

It is interesting to note that two positive peaks of *δM* are observed in the x wt.% $Mn_{55}Bi_{45}$/(1−x) wt.% $Nd_{4.5}Fe_{76.5}Nb_{0.5}B_{18.5}$ (x = 20, 40, 60) magnets. The first peak may represent $Nd_2Fe_{14}B$ hard phase and Fe_3B, α-Fe soft phase interaction in the low applied magnetic field and the second may represent LTP MnBi hard phase and Fe_3B, α-Fe soft phase when the applied field approaches the coercivity of LTP MnBi phase [11]. It is noticed that the strength of the first peak is much higher than the second one. This indicates that interaction between $Nd_2Fe_{14}B$ hard phase and soft phase play a leading role in the exchange coupling. If most soft magnetic phase switches together with the LTP MnBi hard magnetic phase, a higher coercivity will be obtained in the mixed powder.

In order to understand the process of magnetization reversal in detail, the *D*(*H*)-*H* curves have been measured. The *D(H)* is the reduced irreversible portion of magnetization reversal according to the recoil loops and defined as [12, 13]: $D(H) = -\Delta M_{irrev}(H)/2M_r(\infty) = [M_r(\infty) - M_d(H)]/2M_r(\infty)$. According to the model given by Kneller and Hawig [2], the nucleation field H_{no} for irreversible magnetization can be obtained from the maximum of *dD*(*H*)/*dH*-*H* curves shown in Fig. 5. It can be seen clearly that the H_{no} is close to the coercivity H_{cj} for 40 wt.% $Mn_{55}Bi_{45}$/60 wt.% $Nd_{4.5}Fe_{76.5}Nb_{0.5}B_{18.5}$ ($H_{no}/H_{cj} \approx 1$), indicating that most of the soft magnetic phase switches together with the hard magnetic phase at the field amplitude H_{no}. In other words, an effective exchange coupling interaction exists in the sample. While H_{no} is smaller than H_{cj} for 60 wt.% $Mn_{55}Bi_{45}$/40 wt.% $Nd_{4.5}Fe_{76.5}Nb_{0.5}B_{18.5}$ ($H_{no}/H_c \approx 0.78$). It can be supposed that the exchange coupling interaction between the soft and hard phases is weakened, which is consistent with the results of *δM* plots.

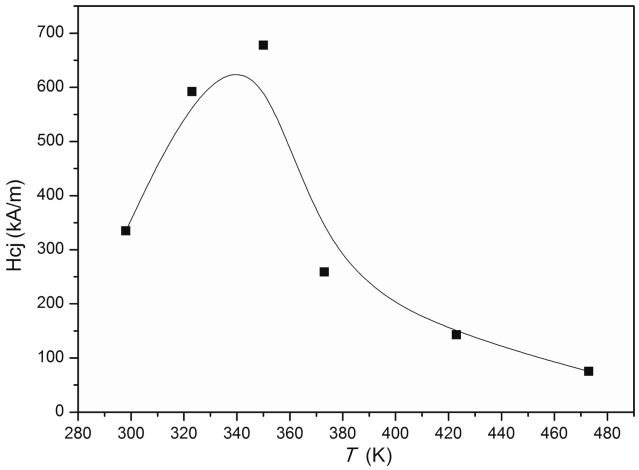

Fig. 6. Dependence of coercivity with temperature for 40 wt.% $Mn_{55}Bi_{45}$/60 wt.% $Nd_{4.5}Fe_{76.5}Nb_{0.5}B_{18.5}$ alloy powder.

Figure 6 shows the dependence of coercivity with temperature for 40 wt.% $Mn_{55}Bi_{45}$/60 wt.% $Nd_{4.5}Fe_{76.5}Nb_{0.5}B_{18.5}$ alloy powder. From 300 K to 350 K, the coercivity increases from 311.2 kA/m to 677.7 kA/m with temperature, the magnet bears a positive temperature coefficient of 2.26 %/K, the negative temperature coefficient of NdFeB alloy is compensated by anomalous temperature dependence of MnBi alloy, which has a positive temperature coefficient of coercivity in the range of 540 K. However, a negative temperature coefficient is still observed above 350 K in the magnet, temperature coefficient of NdFeB alloy is more dominant in the 440

wt.% $Mn_{55}Bi_{45}$/60 wt.% $Nd_{4.5}Fe_{76.5}Nb_{0.5}B_{18.5}$ alloy with the increase of temperature.

4. Summary

The effects of addition of MnBi on microstructure and magnetization behaviors of Fe_3B/$Nd_2Fe_{14}B$-based nanocomposite alloy were investigated. As shown in the XRD results, LTP MnBi and Bi phases accompanied by $Nd_2Fe_{14}B$, Fe_3B and α-Fe phases were observed with the addition of $Mn_{55}Bi_{45}$ alloy. It was found that the coercivity from 192.8 kA/m to 311.2 kA/m with the $Mn_{55}Bi_{45}$ content is 40 wt.%. It was also revealed that saturation magnetization decreased with the additon of MnBi alloy. The δM and D(H)-H plots suggested the occurrence of a stronger exchange-coupling occurring between the hard and soft magnetic phase for the sample with the addition of 40 wt.% $Mn_{55}Bi_{45}$. From 298 K to 350 K, a positive temperature coefficient is founded in 40 wt.% $Mn_{55}Bi_{45}$/60 wt.% $Nd_{4.5}Fe_{76.5}Nb_{0.5}B_{18.5}$ alloy powder, which caused by the addition of $Mn_{55}Bi_{45}$ in the magnet.

Acknowledgments

This work was supported by the National Natural Science Foundation of China (Nos. 51301158 and 51371163) and Provincial Natural Science Foundation (LR15E010001 and LQ15E010005).

References

[1] R. Coehoorn, D. B. de Mooij, J. P. W. B. Duchateau, and K. H. J. Buschow, J. de Phys. **49**, 669 (1988).
[2] S. Hirosawa, Y. Shigemoto, T. Miyoshi, D. Shindo, Y. Park, Y. Gao, and H. Kanekiyo, Scripta. Mater. **48**, 839 (2003).
[3] S. Cao, M. Yue, and Y. X. Yang, J. Appl. Phys. **109**, 07A740 (2011).
[4] J. B. Yang, Y. B. Yang, and X. G. Chen, Appl. Phys. Lett. **99**, 082505 (2011).
[5] Y. B. Yang, X. G. Chen, S. Guo, A. R. Yanb, Q. Z. Huangc, M. M. Wud, D. F. Chend, Y. C. Yanga, and J. B. Yanga, J. Magn. Magn. Mater. **330**, 106, (2013).
[6] J. Cui, J. P. Choi, G. Li, E. Polikarpov, and J. Darsell, J. Appl. Phys. **115**, 17A743 (2014).
[7] M. Sagawa, S. Fujimori, and M. Togawa, J. Appl. Phys. **55**, 2083 (1984).
[8] E. P. Wohlfarth, J. Appl. Phys. **29**, 595 (1958).
[9] H. W. Zhang, C. B. Rong, X. B. Du, J. Zhang, S. Y. Zhang, and B. G. Shen, Appl. Phys. Lett. **82**, 4098 (2003).
[10] P. E. Kelly, K. O. Grady, and P. I. Mayo, IEEE Trans. Magn. **25**, 3881 (1989).
[11] M. X. Pan, P. Y. Zhang, H. L. Ge, N. J. Yu, and W. Qiong, J. Magn. Magn. Mater. **361**, 219 (2014).
[12] J. Zhang, Y. K. Takahashi, R. Gopalan, and K. Hono, Appl. Phys. Lett. **86**, 122509 (2005).
[13] D. Goll, M. Seeger, H. Kronmüller, and J. Bauer, J. Magn. Magn. Mater. **185**, 49 (1998).